Journal of Peptide Science
J. Pept. Sci. 2007; **13**: 287–300
Published online in Wiley InterScience (www.interscience.wiley.com). DOI: 10.1002/psc.839

JOURNAL OF PEPTIDE SCIENCE

Understanding interactions of *gastric inhibitory polypeptide* (GIP) with its G-protein coupled receptor through NMR and molecular modeling

ALPESHKUMAR K. MALDE,[a] SUDHA S. SRIVASTAVA[b] and EVANS C. COUTINHO[a]*

[a] Department of Pharmaceutical Chemistry, Bombay College of Pharmacy, Kalina, Santacruz (E), Mumbai 400 098, India
[b] National Facility for High Field NMR, Tata Institute of Fundamental Research, Homi Bhabha Roda, Navy Nagar, Colaba, Mumbai 400 005, India

Received 6 November 2006; Revised 22 December 2006; Accepted 1 January 2007

Abstract: Gastric inhibitory polypeptide (GIP, or glucose-dependent insulinotropic polypeptide) is a 42-amino acid incretin hormone moderating glucose-induced insulin secretion. Antidiabetic therapy based on GIP holds great promise because of the fact that its insulinotropic action is highly dependent on the level of glucose, overcoming the sideeffects of hypoglycemia associated with the current therapy of Type 2 diabetes. The truncated peptide, GIP(1–30)NH_2, has the same activity as the full length native peptide. We have studied the structure of GIP(1–30)NH_2 and built a model of its G-protein coupled receptor (GPCR). The structure of GIP(1–30)NH_2 in DMSO-d_6 and H_2O has been studied using 2D NMR (total correlation spectroscopy (TOCSY), nuclear overhauser effect spectroscopy (NOESY), double quantum filtered-COSY (DQF-COSY), ^{13}C-heteronuclear single quantum correlation (HSQC) experiments, and its conformation built by MD simulations with the NMR data as constraints. The peptide in DMSO-d_6 exhibits an α-helix between residues Ile12 and Lys30 with a discontinuity at residues Gln19 and Gln20. In H_2O, the α-helix starts at Ile7, breaks off at Gln19, and then continues right through to Lys30. GIP(1–30)NH_2 has all the structural features of peptides belonging to family B1 GPCRs, which are characterized by a coil at the *N*-terminal and a long *C*-terminal α-helix with or without a break. A model of the seven transmembrane (TM) helices of the GIP receptor (GIPR) has been built on the principles of comparative protein modeling, using the crystal structure of bovine rhodopsin as a template. The *N*-terminal domain of GIPR has been constructed from the NMR structure of the *N*-terminal of corticoptropin releasing factor receptor (CRFR), a family B1 GCPR. The intra and extra cellular loops and the *C*-terminal have been modeled from fragments retrieved from the PDB. On the basis of the experimental data available for some members of family B1 GPCRs, four pairs of constraints between GIP(1–30)NH_2 and its receptor were used in the FTDOCK program, to build the complete model of the GIP(1–30)NH_2 : GIPR complex. The model can rationalize the various experimental observations including the potency of the truncated GIP peptide. This work is the first complete model at the atomic level of GIP(1–30)NH_2 and of the complex with its GPCR. Copyright © 2007 European Peptide Society and John Wiley & Sons, Ltd.

Supplementary electronic material for this paper is available in Wiley InterScience at http://www.interscience.wiley.com/jpages/1075-2617/suppmat/

Keywords: diabetes; gastric inhibitory polypeptide (GIP); GIP(1–30)NH_2; GIP receptor (GIPR); 2D NMR; G-protein coupled receptor (GPCR); homology modeling; FTDOCK; MD simulations

INTRODUCTION

Diabetes affects an increasing proportion of populations in both the developed and developing countries and is a major metabolic disorder [1]. Ninety percent of diabetics suffer from Type 2 diabetes. Changing lifestyles, improper eating habits, stress and several unknown factors contribute to the etiology of Type 2 diabetes [2]. The complications of diabetes include hypertension, obesity, fatigue and visual impairment, which affect the socioeconomic status of the individual suffering from diabetes [3]. Present therapy for the treatment of Type 2 diabetes includes insulin, sulphonylureas (e.g. glibenclamide), biguanides (e.g. metformin), acarbose and thiazolidinediones (e.g. pioglitazone). The side effects associated with the current therapy include hypoglycemia, weight gain and liver toxicity [4]. A key component of the pathophysiology of Type 2 diabetes involves a relatively selective defect in the ability of glucose to provoke secretion of insulin from the islets of β-cells in the pancreas. This defect accounts for the failure of the β-cells to compensate for increasing insulin resistance and for the ultimate development of overt hyperglycemia. Sulphonylureas and related compounds stimulate insulin release even in absence of high glucose concentration and this leads to the undesired hypoglycemic side effect. The ideal Type 2 diabetes therapy should have a glucose-dependent insulin release mechanism.

It has been recognized that extracts derived from the gut have a potential to lower blood glucose and this incretin effect is predominantly based on the insulinotropic effect of the incretin hormones: gastric

*Correspondence to: E. C. Coutinho, Department of Pharmaceutical Chemistry, Bombay College of Pharmacy, Kalina, Santacruz (E), Mumbai 400 098, India; e-mail: evans@bcpindia.org

inhibitory polypeptide (GIP) and glucagon-like peptide-1 (GLP-1) [5,6]. GLP-1 derived peptides and synthetic agonists acting on the GLP-1 receptor have demonstrated antidiabetic effects [7]. Given the fact that GLP-1 inhibits gastric emptying in humans to a greater extent than GIP, it is possible that long acting analogs of GIP would be more attractive therapeutically [8]. GIP [9,10] is a 42-amino acid residue peptide (YAEGT^{5}FISDY^{10}SIAMD^{15}KIHQQ^{20}DFVNW^{25}LLAQK^{30} GKKND^{35}WKHNI^{40}TQ). The insulinotropic effects of GIP have been demonstrated in islets of Langerhans, isolated perfused pancreas, and in humans; thus indicating its physiological role as an incretin hormone [11]. While antidiabetic treatment with other insulinotropic agents is limited by the danger of hypoglycemia, a therapy based on GIP is extremely attractive because of the glucose dependency of the insulinotropic action of this hormone. For this reason, GIP is also called glucose-dependent insulinotropic polypeptide. Currently, various attempts to overcome the therapeutic limitations of incretin peptides are under clinical evaluation [12]. Both GIP and GLP-1 are substrates for the proteolytic enzyme – dipeptidyl peptidase IV (DPP IV), which cleaves GIP at the amide bond between Ala2–Glu3, forming GIP(3–42), which is an antagonist at the GIP receptor (GIPR) [13]. Various derivatives have been made, which are resistant to DPP IV and have a longer half-life [14–16].

GIP belongs to the peptide hormone family B1 of G-protein coupled receptors (GPCR) [17]. The other members of this subfamily include glucagon, GLP-1, GLP-2, GHRH, VIP, CRF, parathyroid hormone (PTH), secretin and calcitonin. The peptide in family B1 closest to GIP in terms of sequence homology and biological activity is GLP-1, which is also called a sister hormone of GIP. All GPCRs are characterized by the presence of seven transmembrane (TM) α-helices, three intracellular loops, three extracellular loops, an extracellular *N*-terminal and an intracellular *C*-terminal. There is a disulfide bond between the cysteine residues in the first and the second extracellular loops, which is conserved across all families of GPCR. The family B1 GPCRs are characterized by presence of a large *N*-terminal (~150 residues) with six conserved Cys residues, which form three disulfides by specific pairing of the cysteines [18]. The peptide binding site in this family of GPCRs is located at the extracellular *N*-terminal and the juxta-TM domain formed by the three extracellular loops and the extracellular face of the seven TM helices [19].

Our goal is to study the ligand–receptor interactions at the atomic level in the GIP : GIPR system. Insight into the three-dimensional structure of proteins and peptides and their interactions is of great importance in understanding their function, which can be utilized in drug design. The 3D structure of the *C*-terminal truncated sequence of GIP i.e. GIP(1–30)NH_2 which is equipotent as the full length peptide [20], has been determined by 2D-NMR experiments in solvents DMSO-d_6 and H_2O. In the absence of the porcine GIPR sequence, a model of the human GIPR was built based on principles of comparative protein modeling. The structure of GIP(1–30)NH_2 derived by NMR, was then docked into the model of GIPR using as constraints some experimental data available for family B1 GPCRs. The GIP(1–30)NH_2 : GIPR complex has been thoroughly analyzed to decipher the interactions at the atomic level.

METHODS

Molecular Modeling

All molecular modeling studies were carried out with the modeling programs InsightII (v 2005.L) [21] and Sybyl (v *7.1)* [22] installed on a Pentium-IV PC with the Linux OS (Red Hat Enterprise WS 3.0). The peptide–protein docking was carried out with FTDOCK [23] (v 2.0) running on a Silicon Graphics Fuel workstation with a MIPS R16 000 processor and IRIX 6.5 OS.

NMR Sample Preparation

GIP(1–30)NH_2 (porcine GIP truncated at residue number 30, His18 in human GIP is replaced by Arg in porcine) was purchased from Bachem, UK. Isotopically enriched $^{2}H_2O$ and DMSO-d_6 were from Sigma Chemicals Co., USA. 2,2-Dimethyl-2-silapentan-5-sulfonate (DSS) were from Stohler Isotope Chemicals, USA. For NMR studies, the peptide was dissolved in DMSO-d_6 under an atmosphere of nitrogen to obtain a final concentration of ~2 mM. The same amount was dissolved in 95 : 5 H_2O : D_2O mixture. At this concentration, no aggregation was observed for the peptide in either solvent. This has also been reported for the same peptide and the full length GIP sequence in the literature [24,25]. The pH of the aqueous solution was 3.0. Several other peptides have been studied by NMR at this low pH, including the same peptide in a different solvent [24,26–30]. DSS was used as an internal standard for the two solvents.

NMR Experiments

The NMR experiments were carried out on a Varian Unity Plus 600 MHz and a Bruker Avance 500 (500 MHz) spectrometers. The 1D proton spectra were acquired with a spectral width of 9500 Hz, 64 scans, and digitized with 32 K data points. Water suppression by gradient tailored excitation (WATERGATE) technique was used on the Varian spectrometer for suppressing the water signal [31]. On the Brüker instrument, the powerful technique of Excitation-Sculpting was used [32]. The NMR data was processed using Felix software (v 97) [21].

DOI: 10.1002/psc

The phase sensitive total correlation spectroscopy (TOCSY) [33] and nuclear overhauser effect spectroscopy (NOESY) [34,35] were used for identifying and connecting the spin systems of the individual amino acid residues. The TOCSY spectrum was acquired at 298 K with a spinlock mixing time of 85 ms, using the MLEV-17 sequence [33]. Six NOESY spectra were acquired at 298 K with mixing times of 50, 100, 150, 200, 250 and 300 ms to construct the NOE buildup curves. At the beginning of each experiment, 32 dummy scans were collected to allow the system to reach thermal equilibrium. A total of 2 K data points for 512t_1 values of 32 scans each were acquired. The TOCSY and NOESY spectra were also recorded at temperatures of 298, 308 and 318 K to determine the temperature coefficients of the NH chemical shifts.

Coupling constants ($^3J_{NH\alpha}$) were extracted from a double quantum filtered-COSY (DQF-COSY) [36] spectrum, which was acquired with 96 scans and digitized with 4 K data points in the t_2 dimension. $^1H-^{13}C$ gradient – heteronuclear single quantum correlation (HSQC) [37,38] – experiments with sensitivity enhancement were recorded with 96 transients per t_1 increment to obtain the ^{13}C chemical shifts in both solvents.

Structure Calculation

The pattern of intra and inter residue NOEs, ^1H and ^{13}C chemical shifts, the $^3J_{NH\alpha}$ coupling constants, temperature coefficients of the amide resonances and the chemical shift index (CSI) [39] of the H_α and the C_α resonances were used to draw inferences about the secondary structure of the peptide. Interproton distances calculated from the NOEs were classified, adjusted to preset values (three ranges: 1.8–2.8, 1.8–3.6 and 1.8–5.0 Å) and corrected for methyl, methylene and aromatic rings according to the rules formulated by Wüthrich [40]. The $^3J_{NH\alpha}$ coupling constants were converted to the ϕ values through the modified Karplus equation [41], and introduced as dihedral restraints. The dihedral and distance restraints were incorporated in a simulated annealing (SA) protocol that involved slow heating to 600 K followed by cooling to 300 K in steps of 100 K with a total dynamics run of 25 ps at each stage. The SA procedure was carried out with the Discover module in InsightII (Accelrys Inc., USA). The CFF91 force field [42] with its associated atom potentials and partial charges were used for the simulation. On reaching 300 K, each structure was energy minimized by a combination of steepest descents and conjugate gradients to yield structures with a gradient of 0.001 kcal/mol/Å or lower. The most stable structure amongst these was taken for refinement.

Structure Refinement

The structures generated from the restrained molecular dynamics simulations need to be refined as the distances used as restraints are calculated from NOEs estimated by the isolated spin pair approximation model. Iterative relaxation matrix refinement (IRMA) [43] is a structure refinement tool, which takes into account the entire spin relaxation network and molecular flexibility. A relaxation matrix composed of diagonal and off-diagonal relaxation rates is built based on the distances, the rotational correlation time (τ_c), and the spectrometer frequency. The calculated and experimental NOEs, which reflect the interproton distances are compared, and the structure is iteratively changed until the two converge as closely as possible. The rotational correlation time was estimated from the NOE build up curve of several peaks in the fingerprint region. The refinement is measured by an R factor.

Modeling the GIPR

A model of the GIPR was built using the homology [21] module of InsightII. The potentials and partial charges for all atoms were assigned according to the CFF91 force field [42].

The homology modeling employed here follows a segmented approach [44] where the *N*-terminal, the *C*-terminal, the TM helices (7 TMs), and the loop regions (three intracellular and three extracellular loops) were modeled on separate individual templates. The first step in homology modeling was to build a truncated model (GIPR_T; Step 2 in Scheme 1) of the

Step 1. Derive the structures of GIP(1-30)NH_2 in DMSO-$d_6$and H_2O by 2D NMR

Step 2. Construct a homology model of the GIP receptor without the N-terminal segment (GIPR_T)

Step 3. Build a homology model of the N-terminal (residues 22-138) of the GIP receptor (GIPR_N)

Step 4. Build the GIP(1-30)NH_2:GIPR_N complex through *FTDOCK* and refine by *MULTIDOCK*

Step 5. Associate the GIP(1-30)NH_2:GIPR_N complex with GIPR_T through constraints and refine by simulated annealing (SA)

Step 6. Refine the GIP(1-30)NH_2:GIPR model by SA followed by analysis of all intermolecular interactions

Scheme 1 Sequences of steps in building a model GIP(1–30)NH_2 : GIPR by NMR and molecular modeling.

DOI: 10.1002/psc

GIPR. The amino acid sequence of GIPR was obtained from the NCBI protein database (GI: 4 503 999). The receptor sequence is segmented as follows: residues 1–21 (signal peptide), 22–138 (*N*-terminal), 139–160 (first TM domain TM1), 161–169 (first intracellular loop IC1), 170–189 (TM2), 190–217 (first extracellular loop EC1), 218–241 (TM3), 242–254 (IC2), 255–277 (TM4), 278–294 (EC2), 295–318 (TM5), 319–341 (IC3), 342–359 (TM6), 360–373 (EC3), 374–396 (TM7) and 397–466 (*C*-terminal), based on the literature data [45].

The TM regions (TM1–TM7) and a part of the *C*-terminal were modeled using the crystal structure of bovine rhodopsin (PDB: 1L9H) [46]. TM1–TM7 and the *C*-terminal of GIPR were individually aligned to the respective segments of bovine rhodopsin using ClustalW [47] and the PAM250 [48] scoring matrix. For loop regions, PSI-BLAST [49] was used to search loops that connect two adjacent TM helices; however, no hits were found with an E-value greater than 0.01, probably because the required sequences were too short. The loop regions IC1–IC3, EC1–EC3 and a part of the *C*-terminal were modeled using the 'loop search' utility in the Homology program. The *N*-terminal of GIPR was modeled as a separate entity (GIPR_N; Step 3 in Scheme 1) using the NMR structure (PDB: 1U34) [50] of the *N*-terminal of corticoptropin-releasing factor receptor (CRFR), which is a family B1 GPCR. Sequence alignment of the two *N*-terminal segments was carried out with ClustalW using the PAM250 matrix.

The coordinates of the residues in the TM helices (TM1–TM7) and the *C*-terminal were assigned from the corresponding TMs and the *C*-terminal of bovine rhodopsin. The coordinates of the ICs, ECs and the *C*-terminal were extracted either from the crystal structure or from loops identified in the PDB database. The coordinates of the side chains and backbone atoms were copied to the target sequence only if identical amino acids were found at corresponding positions in the sequence; for 'similar' but not 'identical' amino acids, only the common side chain atoms were copied, while for the rest, amino acid conformations from the InsightII library were used. The side chains of all residues in the model were explored for their optimal conformations, and those with minimum steric clashes (bumps) were assigned to the model. The splice points (the amide groups) were refined by minimization with the CFF91 force field and implemented through Discover (InsightII). The disulfide bond between Cys216 in EC1 and Cys286 in EC2, which is conserved across all GPCR families, was manually created. All the six loops (in the ECs and ICs) and the *C*-terminal segments were refined by an initial minimization with steepest descents followed by conjugate gradients to a gradient convergence of 0.001 kcal/mol/Å. An SA procedure (similar to one discussed above) was then carried out wherein all degrees of freedom for the loops and the *C*-terminal regions were allowed to relax, but the heavy atoms of the other residues (TM1–TM7) were held rigid. The lowest energy structure from the 300 K trajectory was then subjected to a final round of minimization with all heavy atoms tethered by a force constant of 100 kcal/mol/Å [2]. The minimization was done till the gradient converged to 0.001 kcal/mol/Å.

For the *N*-terminal of GIPR (GIPR_N), the coordinates were extracted from the NMR structure of CRFR. There are three conserved disulfides in the *N*-terminal, which is present in all members of family B1 GPCR. The disulfide bond was formed between the pairs: Cys46/Cys70, Cys61/Cys103 and Cys84/Cys118 in the *N*-terminal of GIPR. The final model was subjected to an energy minimization step, with all heavy atoms tethered by a force constant of 50 kcal/mol/Å^2, using steepest descents followed by conjugate gradients.

The bond lengths, bond angles, torsions (ω, ϕ and ψ) and the chirality of the Cα atoms in the constructed models were analyzed with the Prostat module of homology. The Ramachandran map of the two models (GIPR_N and GIPR_T) was plotted and analyzed.

Docking of GIP onto GIPR

The NMR and modeling studies yielded the solution structure of GIP(1–30)NH_2, a model of the *N*-terminal of GIPR (GIPR_N, residues 22–138), and a model of GIPR (GIPR_T, residues 139–466) with the seven TMs, three ECs, three ICs and the *C*-terminal. Experimental studies for GIP, GLP-1 and other related members of family B1 GPCRs, indicate that the peptide hormone binds to its receptor in two steps: in the first step the *C*-terminal of the peptide binds to the extracellular *N*-terminal of the receptor (the affinity step), then in the second step, the *N*-terminal of the peptide binds to the juxta-TM domain (extracellular loops and the extracellular regions of TM helices) leading to intrinsic activity of receptor activation [19].

The FTDOCK algorithm was used to dock the structure of GIP(1–30)NH_2 (obtained by NMR in H_2O) into the homology model of the *N*-terminal of the GIPR (GIPR_N; Step 4 in Scheme 1). The structure of GIP(1–30)NH_2 in water is characterized by a helix spanning residues 7–30, and a random arrangement around residues 1–6 at the *N*-terminal. FTDOCK was run with electrostatics on, a grid size of 0.7 Å and a search over the complete binding space of both molecules. A negative FTDOCK score indicates overlap/interpenetration of the ligand and the receptor – an unfavorable association; a score of zero indicates that the ligand and receptor do not interact at all, while large positive scores denote complex formation with good surface complementarity. The FTDOCK calculations gave rise to 9240 possible complexes. The 'filter' utility in FTDOCK was used to reduce the complexes to a small number, through constraints

DOI: 10.1002/psc

defined at the residue level between the two molecules. The intermolecular constraints between the *C*-terminal of the peptide and the *N*-terminal of GPCR, were taken from the experimental data for family B1 GPCRs. The interface between the two proteins, in the final single complex model obtained after 'filter', was refined at the atomic level using the MULTIDOCK [51] program. The refinement by MULTIDOCK is based on a two step process: (i) a probability based conformational matrix of the protein side chains is refined iteratively by a 'mean-field' method, in which a given side chain interacts with the fixed backbone and the probability weighted average of the surrounding side chains, and (ii) the protein backbone atoms and the highest probability side chain conformations from Step (i) undergo a rigid-body energy minimization to relax the protein interface. Steps (i) and (ii) are repeated until the interaction energy between the two proteins converges.

The next stage involves associating the GIP(1–30)NH_2 : GIPR_N complex with the model of GIPR_T (Step 5 in Scheme 1). The distance constraints between the *N*-terminal of the peptide and the juxta-TM domain of family B1 GPCRs, were assigned between GIPR_T and GIP(1–30)NH_2 in the GIP(1–30)NH_2 : GIPR_N complex. The resulting complex was subjected to an SA protocol where it was slowly heated to 900 K, then cooled to 300 K in steps of 100 K with a dynamics run of 25 ps at each stage. The *C*-terminal of GIP(1–30)NH_2, the complete GIPR_N sequence, the TMs (1–7) of GIPR, the ICs and the *C*-terminal of GIPR were held rigid, while the *N*-terminal of GIP(1–30)NH_2 and EC loops (1–3) of GIPR were kept free in the simulation. The aim was to allow the solution structure of GIP to relax to a reasonable binding configuration in the complex. The distance restraints between the residues of the *N*-terminal of GIP(1–30)NH_2 and the juxta-TM domain of GIPR were applied with a force constant of 100 kcal/mol/Å [2]. On reaching 300 K, each structure was energy minimized by a combination of steepest descents and conjugate gradients to yield structures with a gradient of 0.001 kcal/mol/Å or lower. The TM1 of GIPR_T was then connected to GIPR_N, and this region was optimized using SA as described above. The final GIP(1–30)NH_2 : GIPR complex was carefully analyzed for intermolecular interactions at the residue level.

RESULTS AND DISCUSSIONS

NMR Study

The technique of sequence-specific resonance assignment developed by Wüthrich [52] was used for characterizing the proton spectra of the peptide in the two solvents. Assignments of the protons of all residues were followed by tracing out the backbone connectivities using the NH_i–αH_i peaks in the TOCSY spectrum and the NH_i–αH_{i-1} peaks in the NOESY spectrum. The fingerprint region of the NOESY spectrum of GIP(1–30)NH_2 in DMSO-d_6 and 95% H_2O is given in Figures 1 and 2, respectively. Having assigned the proton resonances, the ^{13}C chemical shifts were assigned from the ^1H–^{13}C HSQC spectrum, which helped resolve any ambiguities in the assignments.

The different secondary structure motifs show specific patterns of sequential, medium range and long range NOEs, thereby giving an insight into the three-dimensional structure of the molecule. Low temperature coefficients of the NH chemical shifts indicate that the amide NH is either intramolecularly hydrogen bonded or solvent shielded. Both these peculiarities are indications of some secondary structural feature. The spatial folding of the peptide chains is also manifest in the proton and the carbon chemical shifts (CSI) [39] as a dispersion of the shifts relative to the random coil structure. Helical regions and stretches containing turns are usually characterized by a continuous stretch of negative deviations ('–1') from the random coil values for the H_α chemical shift, and a positive deviation ('1') in case of $^{13}C_\alpha$ chemical shifts. A β-strand shows exactly the opposite picture.

Interproton distances measured from the linear portion of the NOE build up curves (correlation time, $\tau_c = 100$ ms) and dihedral angles calculated by the modified Karplus equation from

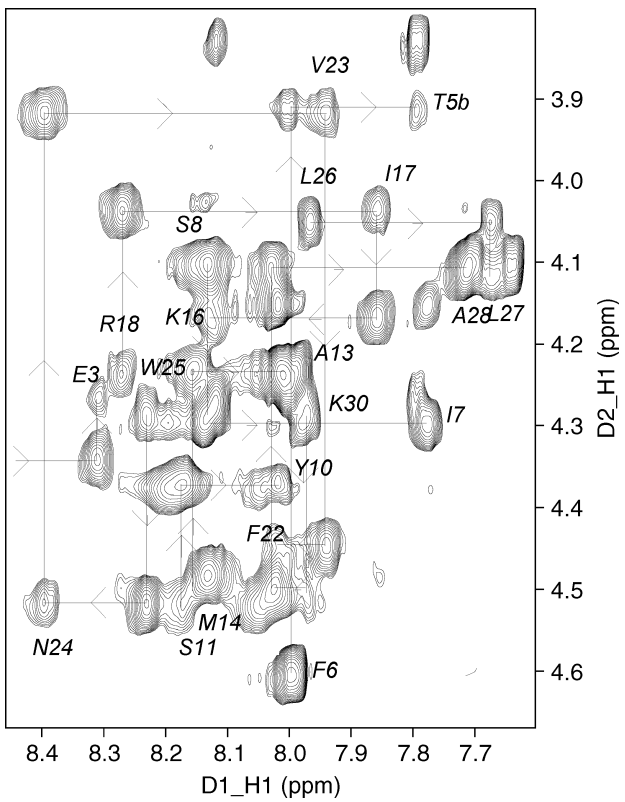

Figure 1 The fingerprint region of the NOESY spectrum (mixing time $\tau_c = 100$ ms) of GIP(1–30)NH_2 in DMSO-d_6.

DOI: 10.1002/psc

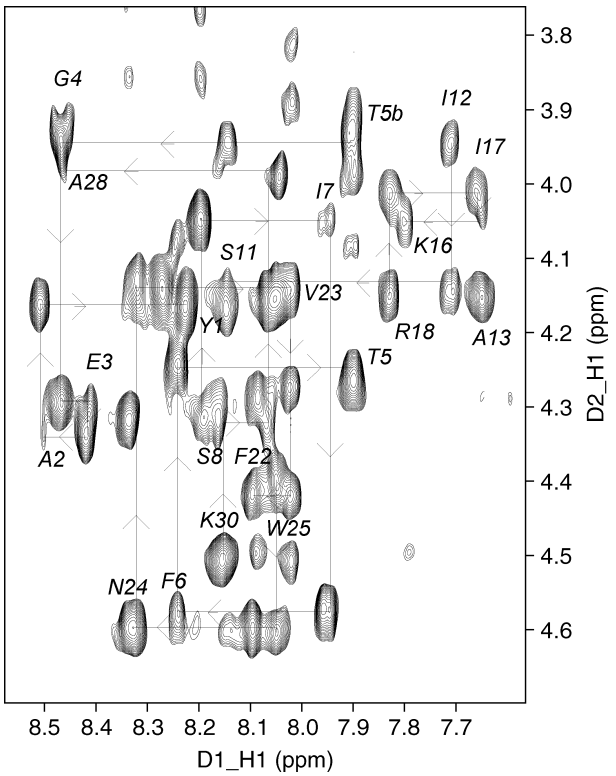

Figure 2 The fingerprint region of the NOESY spectrum (mixing time $\tau_c = 100$ ms) of GIP(1–30)NH_2 in H_2O.

the $^3J_{NH\alpha}$ coupling constants, were introduced as restraints in the MD simulations. The number and type of restraints used in the MD simulations are shown in Table 1. The restraints were satisfied in all the simulations with negligible violations. Further refinement of these simulated structures with IRMA gave conformations relatively free from error.

The final refined structure of GIP(1–30)NH_2 in DMSO-d_6 and H_2O is shown in Figures 3 and 4 respectively.

Table 1 Summary of experimental restraints and statistical analysis of the family of structures of GIP(1–30)NH_2 generated by restrained molecular dynamics simulations

Distance restraints		
All	DMSO-d_6	130
	H_2O	56
Intraresidue	DMSO-d_6	103
	H_2O	37
Interresidue	DMSO-d_6	27
	H_2O	19
Sequential	DMSO-d_6	16
	H_2O	12
NOE violations >0.2 Å	DMSO-d_6	18
	H_2O	8
Ramachandran plot regions (%)		
DMSO-d_6	Favored	85
	Additionally allowed	9
H_2O	Favored	90
	Additionally allowed	6
RMSD of backbone atoms of the ensemble against global minimum structure		
Maximum	DMSO-d_6	1.2
	H_2O	1.9
Minimum	DMSO-d_6	0.2
	H_2O	0.5
Average pair wise	DMSO-d_6	0.8
	H_2O	1.1
IRMA R factor		
	DMSO-d_6	0.68
	H_2O	0.55

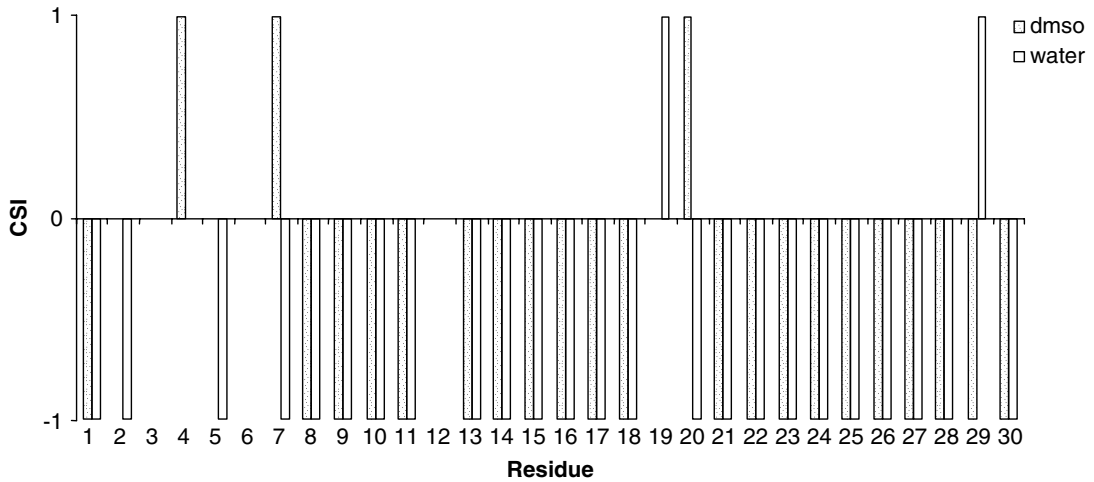

Figure 3 Hα Chemical Shift Index (CSI) analysis of GIP(1–30)NH_2 in DMSO-d_6 and H_2O.

DOI: 10.1002/psc

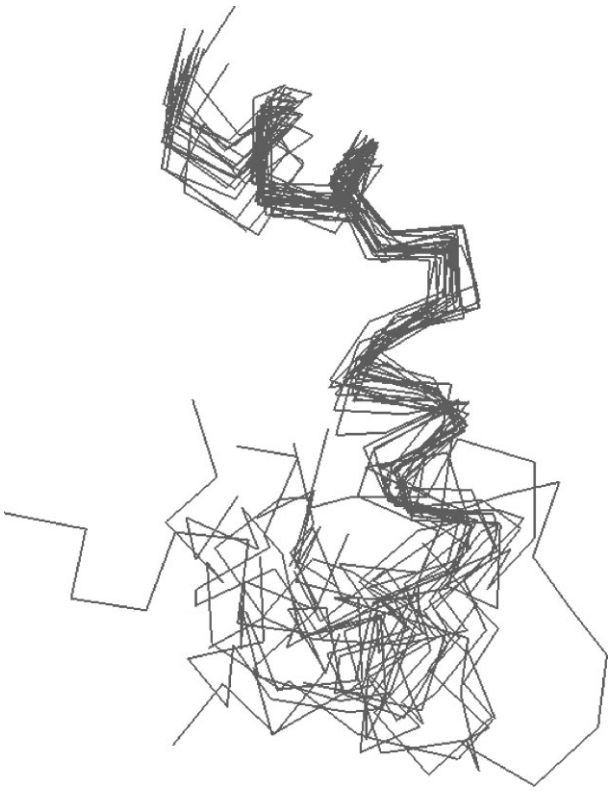

Figure 4 Best fit superposition of the 20 structures of GIP(1–30)NH_2 in DMSO-d_6, between residues 12 and 28. Only bonds between the backbone atoms have been shown. *N*-termini are shown at the bottom.

GIP(1–30)NH_2 in DMSO-d_6

The presence of $d(N,N)_{i,i+1}$, $d(\alpha,N)_{i,i+3}$ and $d(N,N)_{i,i+2}$, connectivity patterns, as well as small $^3J_{NH\alpha}$ coupling constants (~4 Hz), clearly indicate an α-helical character of GIP(1–30)NH_2 in this solvent (Figure S1, Table S1). A structured state is also apparent from the small temperature coefficients ($-\Delta\delta/\Delta T$) of −2.5, −3.0, −3.5 and −2.0 ppb/K for residues Ala13, Ile17, Asp21 and Leu27, respectively. Temperature coefficients of distinguishable amide protons of residues between Ile12 and Lys30 are in the region of −5.0 ppb/K. The CSI (Figure 3) for the H_α protons reads as a continuous stretch of '−1' values from Ile12 to Lys30, with the exception for residues between Gln19 and Gln20. Although CSI shows a continuous stretch of '−1' values between residues 8 and 11, there were no nOe's observed to support a helix in this region. The $^3J_{NH\alpha}$-coupling constant of these residues falls in the range of 3.0–5.0 Hz. All these data show that GIP(1–30)NH_2 in DMSO-d_6 adopts an α-helix between residues Ile12 and Lys30, with a break at residues between Gln19 and Gln20. The initial 11 residues from Tyr1 to Ser11 have a random coil structure. The ensemble of 20 structures is given in Figure 4 and the final refined structure is shown in Figure 5. There are much larger number of NOEs which were used as restraints in DMSO-d_6 compared to H_2O.

GIP(1–30)NH_2 in H_2O

As discussed above, from the pattern of NOEs, the temperature coefficients, the $^3J_{NH\alpha}$ coupling constants and the CSI of H_α protons (Figure S2, Table S2), it can be deduced that GIP(1–30)NH_2 in H_2O exhibits a discontinuous α-helix for the stretch from Ile7 to Lys30 with a kink in the helix at Gln19. The initial six residues from Tyr1 to Phe6 have a random coil structure (Figure 6).

IRAM R factors can be described as the normalized mean deviation between structure factors derived from the model and the experimental data, during the course of the refinement. Thus, the R factor is an indicator of the fit of the structures to the NOE restraints. An R factor close to 0.5 for a medium sized peptide like GIP indicates the structures satisfy the input NOE restraints [26–30]. The R factor of 0.68 in DMSO-d_6 and 0.55 in H_2O are obtained (Table 1).

The CSI analysis (Figure 3) indicates that the chemical shift differences (from the random coil values) for the peptide in the two solvent systems have the same pattern, although the magnitudes of the values are slightly different. Figure 7 shows the superposition of the structures of GIP(1–30)NH_2 in DMSO-d_6 and H_2O. The helical regions of the structures in the two solvents (residues 12–28) lie in the same space. The orientation of the helix beyond residue 20 up to the *C*-terminus is different in the two solvents.

The structure of human GIP(1–30)NH_2 in 50% TFE-d_3 has been reported in the literature [24]. The structure is a continuous α-helix from residues Phe6 to Ala28. TFE is known to strongly promote the formation and stabilization of helical regions in peptides with an intrinsic helical propensity [53]. This explains why in TFE the helical region is continuous without a break, in contrast to the structure in DMSO and water. The structure of the complete human GIP sequence (1–42) in H_2O has also been reported [25] with an α-helical conformation for the midsegment residues Ser11 to Glu29, and a random coil conformation for both the *N*- (residues 1–10) and the *C*- (residues 30–42) termini. The structures of porcine GIP(1–30)NH_2 in DMSO-d_6 and H_2O have a close resemblance to the structure of human GIP(1–30)NH_2 in 50% TFE and to the structure of human GIP(1–42) in water. Many peptide hormones belonging to family B GPCR show similar structural features. Structural studies of peptide hormones similar to GIP, namely GLP-1, exendin-4 and glucagons, in different media, indicate either a continuous α-helical character for the complete peptide sequence or a discontinuous α-helix with a break [54–56]. Thus, for e.g. GLP-1 in TFE adopts an α-helical arrangement extending from residue 7 to 28. The α-helix is however asymmetrically split into two parts at residue 16 [54].

DOI: 10.1002/psc

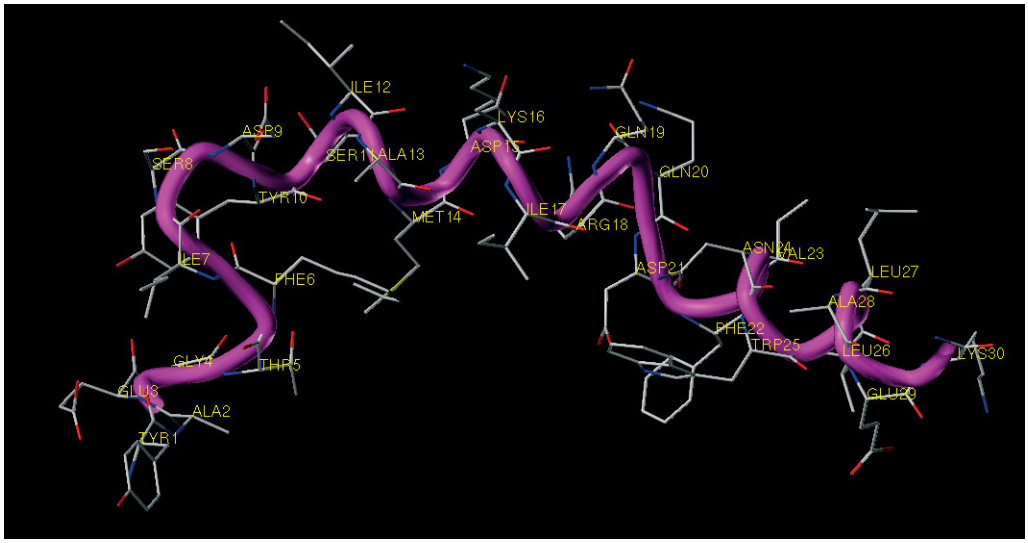

Figure 5 The NMR derived structure of GIP(1–30)NH_2 in DMSO-d_6.

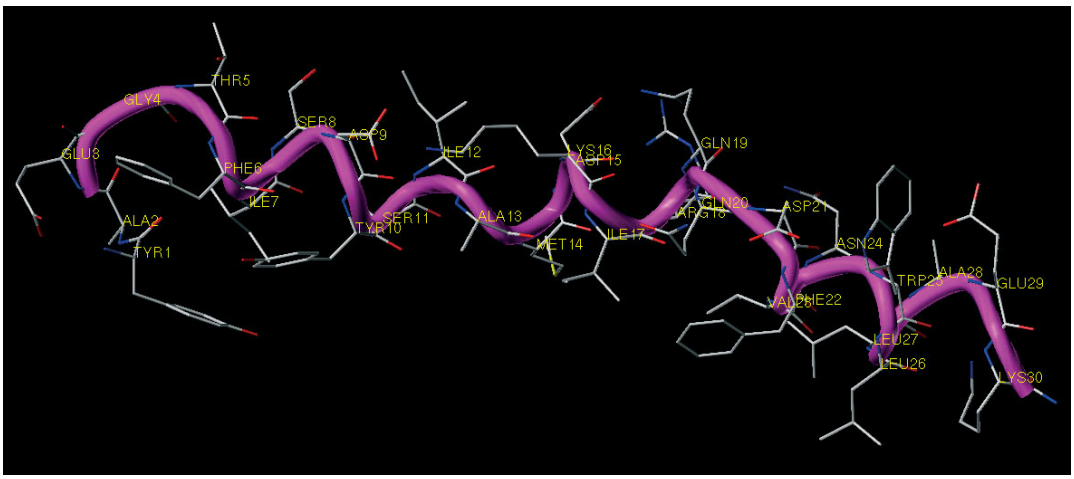

Figure 6 The NMR derived structure of GIP(1–30)NH_2 in H_2O.

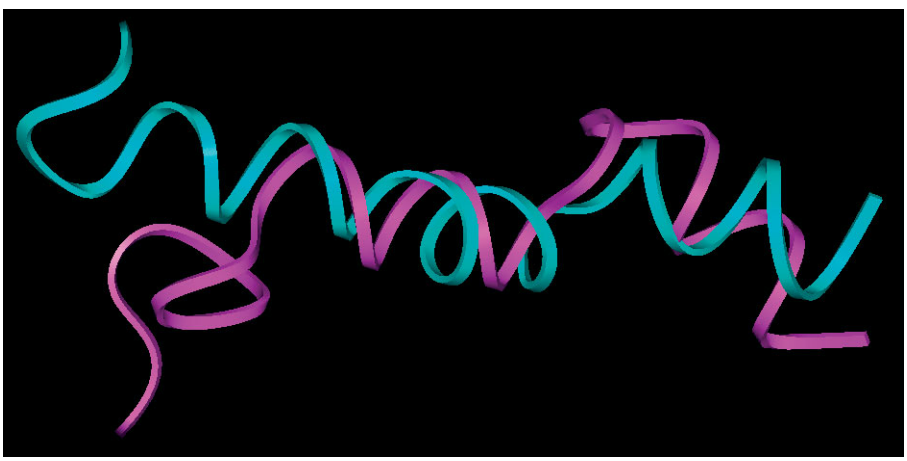

Figure 7 Superposition of NMR structures of GIP(1–30)NH_2 in DMSO-d_6 (magenta) and H_2O (cyan). The ribbon traces the backbone atoms and structures are shown with the *N*-terminal to the left and the *C*-terminal to the right.

DOI: 10.1002/psc

Most studies carried out on the biological relevance of the *N*-terminal region of GIP and related peptides have failed to shed any light on the structural characteristics of this region [57–59]. The present study has also not identified any specific structural feature for the initial residues at the *N*-terminus. However, CD, NMR and X-ray structural studies on family B1 GPCR hormone peptides like GLP-1, exendin-4 and glucagon, show a helical structure as the preferred conformational state for the *N*-terminal region [54–56].

The shorter GIP sequence covering residues 1–30 with the *C*-terminal as amide has the same potency as the full length peptide GIP(1–42). The NMR studies on GIP(1–30)NH_2 in solvents DMSO-d_6 and H_2O and in 50% TFE reveal that the initial few residues (6–10) adopt a random structure, which is followed by a continuous or discontinuous helix that runs through the remaining length of the peptide. GIP(1–42) in H_2O also exhibits a similar structure, with the initial ten residues in a random coil, followed by a helix for the 10–30 segment and terminates with a random coil structure for residues 31–42. The solution structures of the complete and the truncated sequences of GIP shed light on why the full length and truncated peptides have the same potency. The activity of GIP is governed by the α-helical character in the midsegment 30 residues of the peptide and a random coil state for the initial 6–10 residues, which is seen for both the full length and truncated sequences of GIP. The last 12 residues in GIP(1–42) which are absent in the truncated peptide, are in a random coil orientation, and not involved in receptor binding.

```
TM1
1L9H 39-60: MLAAYMFLLIMLGFPINFLTLY
GIPR 139-160: VMYTVGYSLSLATLLLALLILS

TM2
1L9H 73-92: NYILLNLAVADLFMVFGGFT
GIPR 170-189: NYIHINLFTSFMLRAAAILS

TM3
1L9H 112-135: LEGFFATLGGEIALWSLVVLAIER
GIPR 218-241: TAQIVTQYCVGANYTWLLVEGVYL

TM4
1L9H 152-174: HAIMGVAFTWVMALACAAPPLVG
GIPR 255-277: HFRYYLLLGWGAPALFVIPWVIV

TM5
1L9H 204-227: VIYMFVVHFIIPLIVIFFCYGQLV
GIPR 295-318: IWWIIRTPILMTILINFLIFIRIL

TM6
1L9H 261-278: FLICWLPYAGVAFYIFTH
GIPR 342-359: STLTLVPLLGVHEVVFAP

TM7
1L9H 288-310: MTIPAFFAKTSAVYNPVIYIMMN
GIPR 374-396: LGFEIFLSSFQGFLVSVLYCFIN

N-terminal
1U34 15-50 : GSGMKETAAAKFERQHMDSPDLGTTLLEQYCHRTTI
GIPR 22-51 : ------RAETGSKGQTAGELYQRWERYRRECQETLA

1U34 51-86 : GNFSGPYTYCNTTLDQIGTCWPQSAPGALVERPCPE
GIPR 52-86 : AAEPPSGLACNGSFDMY-VCWDYAAPNATARASCPW

1U34 87-122: YFNGIKYNTTRNAYRECLENGTWASRVNYSHCEPIL
GIPR 87-122: YLPWHHHVAAGFVLRQCGSDGQWGLWRDHTQCENPE

1U34 123-133: DD----KQRKYDLHY
GIPR 123-135: KNEAFLDQRLILE--
```

Figure 8 Sequence alignment of the TM regions with 1L9H and the *N*-terminal domain of GIPR with 1U34 structure. The conserved Cys residues in the *N*-terminal domain are shown in boldface.

GIPR Model

The TM regions of bovine rhodopsin (PDB code: 1L9H) exhibits good sequence homology with the TMs of the GIPR. The percentage similarity, which is defined as identical plus conservative substitution, between 1L9H and GIPR for each of the TM regions are TM1 32%; TM2 40%; TM3 33%; TM4 26%; TM5 25%; TM6 30%; and TM7 44% (Figure 8). The overall arrangement of the TMs of GIPR resembles that of bovine rhodopsin. The seven TMs together form a circular bundle of seven helices in the membrane. The loop regions, the ECs and ICs, are random structures with no regular secondary structure definitions. The conserved disulfide bond between EC1 and EC2 confers conformational rigidity to these regions of the receptor, which is confirmed by simulated annealing of the loops. This disulfide linkage is important for ligand binding in many of the GPCRs. The presence of the disulfide bond creates two pseudoloops out of EC2, the first joins TM3 to TM4 and the second connects TM3 to TM5, which ultimately affects the relative orientation of TM4 and TM5, with respect to TM1, TM2 and TM3. The *C*-terminal of GIPR is dominated by two α-helices, the first between residues 403 and 406 and the second between residues 423 and 430; the remaining part of the *C*-terminal is folded as a globular structure.

The *N*-terminal of GIPR (GIPR_N), derived from the NMR structure of the *N*-terminus of CRFR, is dominated by an antiparallel β-sheet comprising residues 79–82 (β1 strand) and 99–102 (β2 strand). The polypeptide fold is stabilized by three disulfide bonds between residues Cys46/Cys70, Cys61/Cys103 and Cys84/Cys118 and by a salt bridge in the center involving Asp66 and Arg101. The conserved residues in the *N*-terminal of family B GPCR are six cysteine residues (Cys46, Cys61, Cys70, Cys84, Cys103 and Cys118 involved in formation of three disulfides), Asp66, Trp71, Pro85 and Trp109; all these are found in the *N*-terminal of both GIPR and CRFR.

GIP(1–30)NH_2 : GIPR Interactions

The structure of GIP(1–30)NH_2 in complex with its receptor was constructed in two steps. First, a model of the GIP(1–30)NH_2 : GIPR_N complex was built

DOI: 10.1002/psc

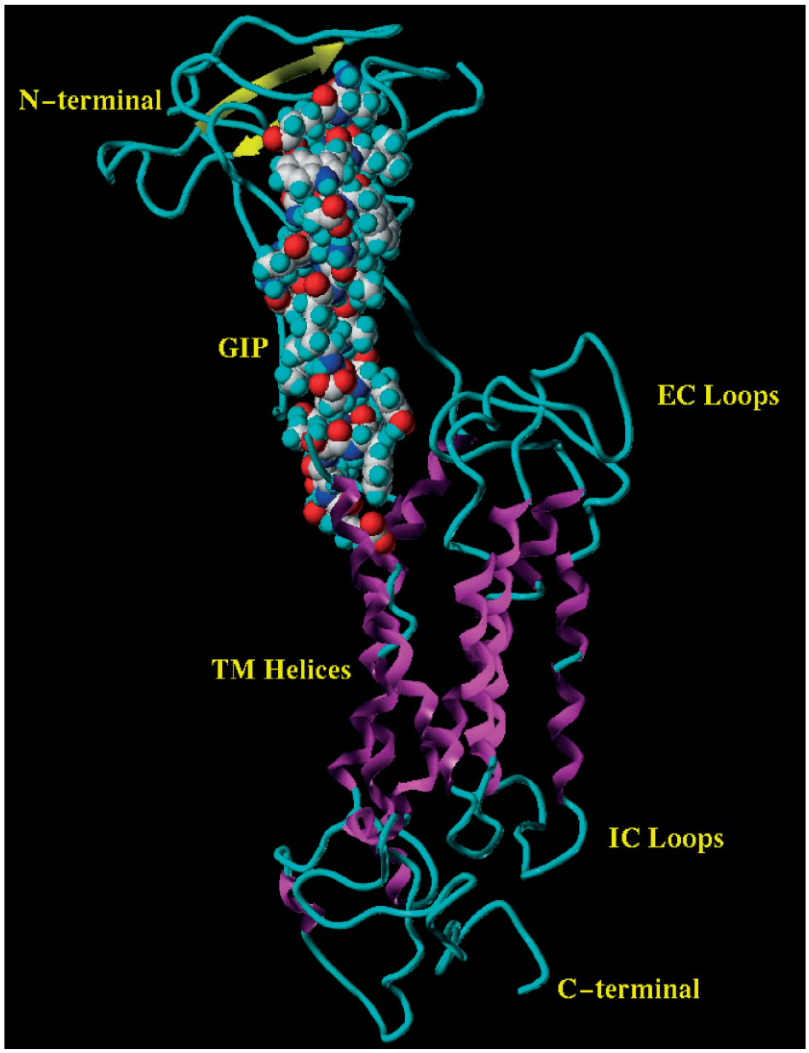

Figure 9 A model of the GIP(1–30)NH_2 : GIPR complex generated using FTDOCK and Simulated Annealing techniques. The TM regions, the *N*-terminal, the IC and EC loops and the *C*-terminal of GIPR are highlighted. The structure of GIP(1–30)NH_2 in the complex is shown as a space filling model.

with FTDOCK, with the *N*-terminal of the receptor interacting with the *C*-terminal of GIP(1–30)NH_2 (Step 4 in Scheme 1). In the next step, the above model of the complex was associated with GIPR_T (GIPR minus GIPR_N) through MD simulations, where the *N*-terminal of GIP(1–30)NH_2 interacts with the juxtamembrane domain of GIPR_T (Step 5 in Scheme 1). This complexation is the first part in the binding (affinity) of the ligand to its receptor.

The docking protocol in FTDOCK employs a geometric surface recognition method, which rapidly scans the translational space of two rigidly rotating molecules. The geometric surface recognition method takes advantage of the fast Fourier transform (FFT) and Fourier correlation theories for rapid scan. Shape complementarity is not the only factor involved in molecular binding. Electrostatic interactions, specifically the charge–charge interactions in the binding interface, also play an important role. The electrostatic complementarity is calculated by Fourier correlation using a simple Coulombic model with a distance-dependent pseudosigmoidal dielectric function. The electrostatic correlation score is used as a binary filter. The false positive geometries that give high shape correlation scores can be excluded if their electrostatic correlation is unfavorable.

Several photoaffinity labeling, site-directed mutagenesis and Ala-scan studies have been carried out across family B GPCRs, which reveal residue level interactions between the ligand and the receptor. Such studies have been reported for secretin [60], PTH [61] (parathyroid hormone), calcitonin [62], CRF [63] CRFR and glucagon [64]. Multiple sequence alignment of these peptides and their receptors with GIP and GIPR, respectively, show several conserved residues for which interactions with the receptor have been reported. In the secretin system, Leu26 of secretin interacts with Leu58 of its receptor

DOI: 10.1002/psc

Table 2 Summary of interactions between GIP(1–30)NH_2 and GIPR as revealed by analysis of the final GIP : GIPR model

GIP(1–30)NH_2	GIPR	Interaction
N-terminal amino	Side chain CO of Glu377	H-bonding
	Backbone CO of Gly375	
NH of Ala2	Side chain CO of Glu377	
side chain CO of Glu3	NH of Gly144	
OH of Thr5	CO of Leu137	
	Backbone NH of Gln138	
	NH of Val139	
OH of Ser8	NH of Leu134	
	NH of Glu135	
Carboxylate of Asp9	Backbone NH of Arg136	
	NH of Leu137	
Arg18 guanido	CO of Arg38	
	CO of Gln37	
Glu3 carboxylate	Arg190 guanidino	Salt bridge
Asp15 carboxylate	Arg136 guanidino	
Tyr1 side chain	Leu374 side chain	Hydrophobic
Phe6 side chain	Tyr141 side chain	
Met14 side chain	Leu35 side chain	
Ile17 side chain	Leu35 side chain	
Leu26 side chain	Leu50 side chain	
Lys30 side chain	Leu50 side chain	

and Arg18 of the ligand interacts with Arg36 of its receptor [60]. The corresponding residues in GIP(1–30)NH_2 : GIPR system are Leu26(GIP(1–30)NH_2):Leu50(GIPR) and His18(GIP(1–30)NH_2):Arg38(GIPR). These represent the interaction between the *C*-terminal of the peptide and the *N*-terminal of the receptor leading to initial binding (*affinity*). These pairs of interactions were used as constraints to filter the large number of GIP(1–30)NH_2 : GIPR_N complexes generated by FTDOCK, from which one unique complex was extracted.

Several important interactions contribute to the stability of the GIP(1–30)NH_2 : GIPR_N complex – a hydrogen bond between the guanidino group of Arg18(GIP(1–30)NH_2) with the backbone carbonyls of Arg38(GIPR_N) and Gln37(GIPR_N) and hydrophobic interactions between the side chains Met14(GIP(1–30)NH_2):Leu35(GIPR_N), Ile17(GIP(1–30)NH_2):Leu35(GIPR_N),Leu26(GIP(1–30)NH_2):Leu50(GIPR_N), and Lys30 (GIP(1–30)NH_2):Leu50(GIPR_N). Thus, majority of the interactions between the *C*-terminal of GIP(1–30)NH_2 and the *N*-terminal of GIPR (GIPR_N) are hydrophobic in nature and essentially involve residues within the α-helix segment of GIP(1–30)NH_2.

The GIP sequences lacking the first six or seven residues in the *N*-terminal i.e. GIP(6–30)NH_2 and GIP(7–30)NH_2 have been reported as antagonists of GIPR [65]. These two truncated peptides also adopt an α-helical structure and interact like GIP(1–30)NH_2 with the *N*-terminal of GIPR (GIPR_N). However, the residues responsible for the intrinsic activity (the *N*-terminal residues of the peptide) which interact with the juxta-TM domain of GIPR are absent causing them to act as anatagonists at the receptor.

The antagonistic nature of GIP sequences lacking the initial *N*-terminal residues is also highlighted by other studies. Thus, the Ala-scan for first seven residues of GIP shows the importance of the third residue (Glu3) in its activity [53]. The Glu3Pro GIP mutant is a potent GIPR antagonist, again pinpointing Glu3 in GIP as vital in modulating its biological activity [66]. Finally, the truncated GIP(3–42) sequence formed by cleavage at the Ala2–Glu3 amide bond by DPP IV is an antagonist of GIPR. All these sequences lack the initial amino acids, which are vital for intrinsic activity by interacting with the juxta-TM domain of GIPR_T.

That Gln3 interacts with Lys187 in its receptor is revealed by a site-directed mutagenesis study involving the Gln3Asp glucagon mutant and the Lys187Arg receptor mutant [67]. The corresponding interaction in the GIP system is Glu3(GIP(1–30)NH_2):Arg190(GIPR). Further, Ala8 of GLP-1 interacts with Glu387 in its GLP-1 receptor as discovered by a site-directed mutagenesis study [64]. The corresponding interaction in the GIP system is Ala2(GIP(1–30)NH_2):Glu377(GIPR). These two constraints involving Glu3 and Ala2 were placed between the GIP(1–30)NH_2 : GIPR_N complex and the GIPR_T model and subjected to a MD simulation to find the best configuration for the final complete GIP(1–30)NH_2 : GIPR model (Figure 9).

The RMSD of the heavy atoms of GIP(1–30)NH_2 between the solution and receptor bound states is 2.25;

DOI: 10.1002/psc

this indicates that the peptide has undergone a significant conformational change upon binding to its receptor. Analysis of the final model reveals several important interactions between GIP(1–30)NH_2 and its receptor (Table 2), in addition to those discussed above between the GIPR_N and the *C*-terminal of GIP(1–30)NH_2. The majority of the interactions between the *N*-terminal of GIP(1–30)NH_2 and the juxta-membrane domain of GIPR are ionic and polar in nature. The GIP(1–30)NH_2 : GIPR model gives deep insights into the ligand–receptor interactions at the atomic level which was hitherto unavailable.

CONCLUSIONS

One of the promising therapies for diabetes is based on GIP, a 42 amino acid incretin hormone secreted in response to high glucose levels. Therapy with GIP has several advantages over the related incretin hormone GLP-1, because of the fact that GLP-1 besides its incretin effects is a relatively stronger inhibitor of gastric emptying in humans than GIP. The major disadvantage with GIP is its short half-life, being a substrate for DPP IV that cleaves it at the Ala2–Glu3 amide bond forming the truncated GIP(3–42) sequence, which is an antagonist. GIP is a member of the family B1 of GPCR. The truncated peptide GIP(1–30)NH_2 retains the activity of the full length peptide. We have studied the binding of GIP(1–30)NH_2 with its receptor GIPR at the atomic level using NMR and molecular modeling techniques. The solution structure of GIP(1–30)NH_2 has been built from by 2D NMR studies in DMSO-d_6 and H_2O. In DMSO-d_6, GIP(1–30)NH_2 assumes an α-helix between residues Ile12 and Lys30, with a discontinuity at Gln19 and Gln20. In H_2O, the α-helix commences from Ile7, breaks at Gln19 and continues up to the *C*-terminal end Lys30. GIP(1–30)NH_2 has all the essential structural features of family B1 GPCR peptide hormones – GLP-1, exendin-4 and glucagon; which are all characterized by an *N*-terminal random coil structure followed by a long α-helix with or without a discontinuity. The complete model of the GIPR has been built using a segmented approach, where the TM helices, the *N*-terminal, the intra and extracellular loops and the *C*-terminal were modeled based on different templates. A model of the GIP(1–30)NH_2 : GIPR complex has been built using four pairs of constraints (common across the family B1 GPCRs) with the program FTDOCK followed by a refinement with a Simulated Annealing procedure. The model explains the equipotency of GIP(1–30)NH_2 with the full length sequence. The main events in the binding process are: first an interaction between the *C*-terminal of the peptide (residues 7–30) and the *N*-terminal of GIPR; which is followed by interaction of the *N*-terminal of the peptide (residues 1–6) with the juxta-TM domain of the receptor. The model also explains why GIP(6–30)NH_2 and GIP(7–30)NH_2 are antagonists of GIP. The interactions between GIP(1–30)NH_2 and its receptor gives insights into the molecular recognition process and this information can be fruitfully exploited for design of more potent peptides and structure-based drug design of nonpeptide mimetics. This is a first complete model of GIP(1–30)NH_2 and its interaction with its G-protein coupled receptor.

Supplementary Material

Supplementary electronic material for this paper is available in Wiley InterScience at: http://www.interscience.wiley.com/jpages/1075-2617/suppmat/

Acknowledgements

This work was supported by the Department of Science and Technology (DST), New Delhi through grants SR/S0/BB-10/2005 and SR/FST/LS1-163/2003 to ECC. AKM thanks Council of Scientific and Industrial Research (CSIR), New Delhi for financial support. The facilities provided by the National Facility for High Field NMR located at TIFR are greatly acknowledged.

The coordinates of the solution structures of GIP(1–30)NH_2 in DMSO-d_6 and 95% H_2O, and the complete GIP : GIPR complex are available on request from authors.

REFERENCES

1. Sarabu R, Tilley J. Recent advances in therapeutic approaches to Type 2 Diabetes. *Annu. Rep. Med. Chem.* 2004; **39**: 39–56.
2. Zimmet P, Alberti KG, Shaw J. Global and societal implications of the diabetes epidemic. *Nature* 2001; **414**: 782–787.
3. Zhang B, Moller DE. New approaches in the treatment of type 2 diabetes. *Curr. Opin. Chem. Biol.* 2000; **4**: 461–467.
4. Moller DE. New drug targets for type 2 diabetes and the metabolic syndrome. *Nature* 2001; **414**: 821–827.
5. Kieffer TJ. GIP or not GIP? That is the question. *Trends Pharmacol. Sci.* 2003; **24**: 110–112.
6. Vella A, Rizza RA. New insights into the regulation of glucagon secretion by glucagon-like peptide-1. *Horm. Metab. Res.* 2004; **36**: 822–829.
7. Holz GG, Chepurny OG. Glucagon-like peptide-1 synthetic analogs: new therapeutic agents for use in the treatment of diabetes mellitus. *Curr. Med. Chem.* 2003; **10**: 2471–2483.
8. Irwin N, Green BD, Gault VA, Greer B, Harriott P, Bailey CJ, Flatt PR, O'Harte PM. Degradation, insulin secretion and antihyperglycemic actions of two palmitate-derivitized N-terminal pyroglutamyl analogues of glucose-dependent insulinotropic polypeptide. *J. Med. Chem.* 2005; **48**: 1244–1250.
9. Moody AJ, Thim L, Valverde I. Isolation and sequencing of human gastric inhibitory peptide (GIP). *FEBS* 1984; **172**: 142–148.
10. Brown JC, Dryburgh JR. A gastric inhibitory polypeptide. II. The complete amino acid sequence. *Can. J. Biochem.* 1971; **49**: 867–872.
11. Meier JJ, Nauck MA, Schmidt WE, Gallwitz B. Gastric inhibitory polypeptide: the neglected incretin revisited. *Regul. Pept.* 2002; **107**: 1–13.
12. Meier JJ, Gallwitz B, Nauck MA. Glucagon-Like peptide 1 and gastric inhibitory polypeptide: potential applications in Type 2 diabetes mellitus. *BioDrugs* 2003; **17**: 93–102.

13. Gault VA, Parker JC, Harriott P, Flatt PR, O'Harte FP. Evidence that the major degradation product of glucose-dependent insulinotropic polypeptide, GIP(3–42), is a GIP receptor antagonist in vivo. *J. Endocrinol.* 2002; **175**: 525–533.
14. O'Harte FPM, Gault VA, Parker JC, Harriott P, Mooney MH, Bailey CJ, Flatt PR. Improved stability, insulin-releasing activity and antidiabetic potential of two novel N-terminal analogues of gastric inhibitory polypeptide: N-acetyl-GIP and pGlu-GIP. *Diabetologia* 2002; **45**: 1281–1291.
15. Gault VA, Flatt PR, Bailey CJ, Harriott P, Greer B, Mooney MH, O'Harte FPM. Enhanced cAMP generation and insulin-releasing potency of two novel Tyr1-modified enzyme-resistant forms of glucose-dependent insulinotropic polypeptide is associated with significant antihyperglycaemic activity in spontaneous obesity-diabetes. *Biochem. J.* 2002; **367**: 913–920.
16. Gault VA, Irwin N, Harriott P, Flatt PR, O'Harte FPM. DPP IV resistance and insulin releasing activity of a novel di-substituted analogue of glucose-dependent insulinotropic polypeptide, (Ser2-Asp13)GIP. *Cell Biol. Int.* 2003; **27**: 41–46.
17. Gether U. Uncovering molecular mechanisms involved in activation of G protein-coupled receptors. *Endocr. Rev.* 2000; **21**: 90–113.
18. Harmer AJ. Family-B G-protein-coupled receptors. *Genome Biol.* 2001; **2**: 3013.1–3013.10.
19. Hoare SRJ. Mechanisms of peptide and nonpeptide ligand binding to class B G-protein-coupled receptors. *Drug Discov. Today* 2005; **10**: 417–427.
20. Fehmann HC, Goke B. Characterization of GIP(1–30) and GIP(1–42) as. stimulators of proinsulin gene transcription. *Peptides* 1995; **16**: 1149–1152.
21. Insight-II 2005, Felix 97, Accelrys Inc. San Diego, CA, USA.
22. Sybyl 7.1, Tripos Associates Inc., 1699 S Hanley Rd., St. Louis, MO 631444, USA.
23. Gabb HA, Jackson RM, Sternberg MJE. Modelling protein docking using shape complementarity, electrostatics and biochemical information. *J. Mol. Biol.* 1997; **272**: 106–120.
24. Alana I, Hewage CM, Malthouse JPG, Parker JC, Gault VA, O'Harte FPM. NMR structure of the glucose-dependent insulinotropic polypeptide fragment, GIP(1–30)amide. *Biochem. Biophys. Res. Commun.* 2004; **325**: 281–286.
25. Alana I, Parker JC, Gault VA, Flatt PR, O'Harte FPM, Malthouse JPG, Hewage CM. NMR and alanine scan studies of glucose-dependent insulinotropic polypeptide in water. *J. Biol. Chem.* 2006; **281**: 16370–16376.
26. Prabhu A, Malde A, Srivastava S, Coutinho E. Solution conformation of substance P antagonists,[D-Arg^{1}, D-Trp^{7,9}, Leu^{11}]-SP, [D-Arg^{1}, D-Pro^{2}, D-Trp^{7,9}, Leu^{11}]-SP and [D-Pro^{2}, D-Trp^{7,9}]-SP by CD, NMR and MD simulations. *Peptides* 2005; **26**: 875–885.
27. Kanyalkar M, Srivastava S, Coutinho E. Conformation of N-terminal HIV-1 tat (fragment 1–9) peptide by NMR and MD simulations. *J. Pept. Sci.* 2001; **7**: 579–587.
28. Tauro S, Coutinho E, Srivastava S. Conformation of the peptide antibiotic–histatin 8 in aqueous and non aqueous media. *Lett. Pept. Sci.* 2001; **8**: 295–307.
29. Desai P, Coutinho E, Srivastava S, Haq W, Katti SB. Conformation of an immunoreactive undecapeptide fragment (10–20) of Asp ϕ1 by NMR and molecular modeling. *Lett. Pept. Sci.* 2002; **9**: 21–34.
30. Desai P, Coutinho E, Srivastava S. Conformational diversity of T-kinin in DMSO, water and HFA. *Eur. J. Med. Chem.* 2002; **37**: 135–146.
31. Sklenar V, Piotto M, Leppik K, Saudek V. Gradient-tailored water suppression for 1H-15N HSQCJ experiments optimized to retain full sensitivity. *J. Magn. Reson. A* 1993; **102**: 241–245.
32. Hwang TL, Shaka AJ. Water suppression that works. Excitation sculpting using arbitrary waveforms and pulsed field gradients. *J. Magn. Reson. A* 1995; **112**: 275–279.
33. Bax A, Davis DG. MLEV-17 based two-dimensional homonuclear magnetization transfer spectroscopy. *J. Magn. Reson.* 1985; **65**: 355–360.
34. Jeener J, Meier BH, Bachman P, Ernst RR. Investigation of exchange processes by two-dimensional NMR spectroscopy. *J. Chem. Phys.* 1979; **71**: 4546–4553.
35. Wagner R, Berger S. Gradient-selected NOESY–a fourfold reduction of the measurement time for the NOESY experiment. *J. Magn. Reson.* 1996; **123A**: 119–121.
36. Derome AE, Williamson MP. Rapid-pulsing artifacts in double quantum filtered COSY. *J. Magn. Reson.* 1990; **88**: 177–185.
37. Kay LE, Keifer P, Saarinen T. Pure absorption gradient enhanced heteronuclear single quantum correlation spectroscopy with improved sensitivity. *J. Am. Chem. Soc.* 1992; **114**: 10663–10665.
38. Palmer AG III, Cavanagh J, Wright PE, Rance M. Sensitivity improvement in proton-detected two-dimensional heteronuclear correlation NMR spectroscopy. *J. Magn. Reson.* 1991; **93**: 151–170.
39. Wishart DS, Sykes BD, Richards FM. The chemical shift index: a fast and simple method for the assessment of protein secondary structure through NMR spectroscopy. *Biochemistry* 1992; **31**: 1647–1651.
40. Wüthrich K. *NMR of Proteins and Nucleic Acids*. Wiley: New York, 1986.
41. Vuister GW, Bax A. Quantitative J correlation: a new approach for measuring homonuclear three-bond J (HNHα) coupling constants in 15 N-enriched proteins. *J. Am. Chem. Soc.* 1993; **115**: 7772–7777.
42. Maple J, Dinur U, Hagler AT. Derivation of force fields for molecular mechanics and dynamics from ab initio energy surfaces. *Proc. Natl. Acad. Sci. U.S.A.* 1988; **85**: 5350–5354.
43. NMRchitect User Guide, version 2.3, Biosym Technologies, San Diego, 1993.
44. Khedkar SA, Malde AK, Coutinho EC. Modeling human Neurokinin-1 receptor structure using the crystal structure of bovine rhodopsin. *Internet Electron. J. Mol. Des.* 2005; **4**: 329–341.
45. Volz A, Göke R, Lankat-Buttgereit B, Fehmann H, Bode HP, Göke B. Molecular cloning, functional expression, and signal transduction of the GIP-receptor cloned from a human insulinoma. *FEBS Lett.* 1995; **373**: 23–29.
46. Okada T, Fujiyoshi Y, Silow M, Navarro J, Landau EM, Shichida Y. Functional role of internal water molecules in rhodopsin revealed by x-ray crystallography. *Proc. Natl. Acad. Sci. U.S.A.* 2002; **99**: 5982–5987.
47. Thompson JD, Higgins DG, Gibson TJ. CLUSTAL W: improving the sensitivity of progressive multiple sequence alignment through sequence weighting, positions-specific gap penalties and weight matrix choice. *Nucleic Acid Res.* 1994; **22**: 4673–4680.
48. Dayhoff MO, Barker WC, Hunt LT. Establishing homologies in protein sequences. *Meth. Enzymol.* 1983; **91**: 524–544.
49. Altschul SF, Madden TL, Schäffer AA, Zhang J, Zhang Z, Miller W, Lipman DJ. Gapped BLAST and PSI-BLAST: a new generation of protein database search programs. *Nucleic Acid Res.* 1997; **25**: 3389–3402.
50. Grace CRR, Perrin MH, DiGruccio MR, Miller CL, Rivier JE, Vale WW, Riek R. NMR structure and peptide hormone binding site of the first extracellular domain of a type B1 G protein-coupled receptor. *Proc. Natl. Acad. Sci. U.S.A.* 2004; **101**: 12836–12841.
51. Jackson RM, Gabb HA, Sternberg MJE. Rapid refinement of protein interfaces incorporating solvation: application to the docking problem. *J. Mol. Biol.* 1998; **276**: 265–285.
52. Wüthrich K, Billeter M, Braun W. Polypeptide secondary structure determination by nuclear magnetic resonance observation of short proton-proton distances. *J. Mol. Biol.* 1984; **180**: 715–740.
53. Khandelwal P, Seth S, Hosur RV. CD and NMR investigations on trifluoroethanol-induced step-wise folding of helical segment from scorpion neurotoxin. *Eur. J. Biochem.* 1999; **264**: 468–478.
54. Chang X, Keller D, Bjorn S, Led JJ. Structure and folding of glucagon-like peptide 1-7-(7–36)-amide in aqueous trifluoroethanol studied by NMR. *Magn. Reson. Chem.* 2001; **39**: 477–483.
55. Andersen NH, Brodsky Y, Neidigh JW, Prickett KS. Medium-dependence of the secondary structure ofexendin-4 and glucagon-like-peptide-1. *Bioorg. Med. Chem.* 2002; **10**: 79–85.

56. Braun W, Wider G, Lee KH, Wüthrich K. Conformation of glucagon in a lipid-water interphase by 1H nuclear magnetic resonance. *J. Mol. Biol.* 1983; **169**: 921–948.
57. Manhart S, Hinke SA, McIntosh CH, Pederson RA, Demuth HU. Structure-function analysis of a series of novel GIP analogues containing different helical length linkers. *Biochemistry* 2003; **42**: 3081–3088.
58. Gallwitz B, Witt M, Morys-Wortmann C, Folsch UR, Schmidt WE. GLP-1/GIP chimeric peptides define the structural requirements for specific ligand-receptor interaction of GLP-1. *Regul. Pept.* 1996; **63**: 17–22.
59. Hinke SA, Manhart S, Pamir N, Demuth H, Gelling RW, Pederson RA, McIntosh CHS. Identification of a bioactive domain in the amino-terminus of Glucose-dependent Insulinotropic Polypeptide (GIP). *Biochem. Biophys. Acta* 2001; **1547**: 143–155.
60. Dong M, Li Z, Zang M, Pinon DI, Lybrand TP, Miller LJ. Spatial approximation between two residues in the mid-region of secretin and the amino terminus of its receptor: incorporation of seven sets of such constraints into a three-dimensional model of the agonist-bound secretin receptor. *J. Biol. Chem.* 2003; **278**: 48300–48312.
61. Gensure RC, Carter PH, Petroni BD, Juppner H, Gardella TJ. Identification of determinants of inverse agonism in a constitutively active parathyroid hormone/parathyroid hormone-related peptide receptor by photoaffinity cross-linking and mutational analysis. *J. Biol. Chem.* 2001; **276**: 42692–42699.
62. Dong M, Pinon DI, Cox RF, Miller LJ. Importance of the amino terminus in secretin family G protein-coupled receptors: intrinsic photoaffinity labeling establishes initial docking constraints for the calcitonin receptor. *J. Biol. Chem.* 2004; **279**: 1167–1175.
63. Klose JA, Fechner K, Beyermann M, Krause E, Wendt N, Bienert M, Rudolph R, Rothemund S. Impact of N-terminal domains for corticotropin-releasing factor (CRF) receptor-ligand interactions. *Biochemistry* 2005; **44**: 1614–1623.
64. Runge S, Gram C, Brauner-Osborne H, Madsen K, Knudsen LB, Wulff BS. Three distinct epitopes on the extracellular face of the glucagon receptor determine specificity for the glucagon amino terminus. *J. Biol. Chem.* 2003; **278**: 28005–28010.
65. Gelling RW, Coy DH, Pederson RA, Wheeler MB, Honke S, Kwan T, McIntosh CHS. GIP(6-30amide) contains the high affinity binding region of GIP and is a potent inhibitor of GIP1-42 action in vitro. *Regul. Pept.* 1997; **69**: 151–154.
66. Gault VA, O'Harte FPM, Harriott P, Flatt PR. Characterization of the cellular and metabolic effects of a novel enzyme-resistant antagonist of glucose-dependent insulinotropic polypeptide. *Biophys. Biochem. Res. Commun.* 2002; **290**: 1420–1426.
67. Perret J, Van Craenenbroeck M, Langer I, Vertongen P, Gregoire F, Robberecht P, Waelbroeck M. Mutational analysis of the glucagon receptor: similarities with the vasoactive intestinal peptide (VIP)/pituitary adenylate cyclase-activating peptide (PACAP)/secretin receptors for recognition of the ligand's third residue. *Biochem. J.* 2002; **362**: 389–394.

DOI: 10.1002/psc